PCCP

Accepted Manuscript

ROYAL SOCIETY OF CHEMISTRY

www.rsc.org/pccp

Physical Chemistry Chemical Physics RSCPublishing

COMMUNICATION

Towards Fibrous Woven Memory from All-Carbon Electronic Fibers

Cite this: DOI: 10.1039/x0xx00000x

Ru Li,[a,b] Rui Sun,[a] Yanyan Sun,[a] Peng Gao,[a] Yongyizhang,[a] Zhongming Zeng[a] and Qingwen Li[a]

Received ooth January 2012,
Accepted ooth January 2012

DOI: 10.1039/x0xx00000x

www.rsc.org/

Fibrous all-carbon woven memory has been formed by using reduced acid graphene oxide as switching materials, and flexible carbon nanotube fibers as electrodes. The as prepared fibrous all-carbon woven memory exhibited ultra-high ON/OFF current ratio of 10^9, fast switching speed of 3 ms, and long life time at least 500 cycles that could pave the way for future e-textiles.

Integration of electronic functions within fabrics, including wire-shaped transistors,[1, 2] lithium-ion battery,[3] supercapacitor,[4] fibrous solar cells[5, 6] and woven memory etc.,[7] shows great promise in developing wearable and smart e-textiles, among which the fibrous memory will be particularly promising to be the fundamental component of e-textiles with intelligent storage ability for codes or data.[8] Recently, it has been revealed that carbon materials including graphene,[9, 10] graphene oxide,[11, 12] graphite[13, 14] or amorphous carbon[15] are interesting materials for fabricating nonvolatile carbon memories with ON/OFF ratio $>10^6$ and operation time ~ 1 us. In general, such carbon memories are fabricated with active carbonous components sandwiched or deposited between two rigid metal electrodes on SiO_2/Si substrate,[9-11, 13, 14, 16-18] making it difficult to be flexible and integrated into fabrics. On this aspect, carbon nanotube fibers,[19, 20] which are mechanically strong, conducting, highly flexible and knittable, may open up access to serve as not only an ideal alternative for rigid electrodes, but also functional interfaces for designing and developing a variety of fibrous devices.[3, 7, 21]

In this report, the double-walled carbon nanotube (DWNT) fiber directly spun from a spinnable array is used as flexible conducting electrode,[22] heat reduced acid graphene oxide (rGO) employed as active carbon material is coated on the outer surface of DWNT fiber, a conformal all-carbon based structure with controllable fiber diameter and rGO coating thickness is obtained and defined as DWNT@rGO fiber. By cross-stacking the two DWNT@rGO fibers at a right angle, a fibrous all-carbon woven memory for data storage is successfully demonstrated. Although with simple device configuration, the fibrous memory shows exciting performance with ultra-high ON/OFF current ratio of 10^9 and fast switching response. Importantly, such memory is knittable and therefore applicable for smart textile.

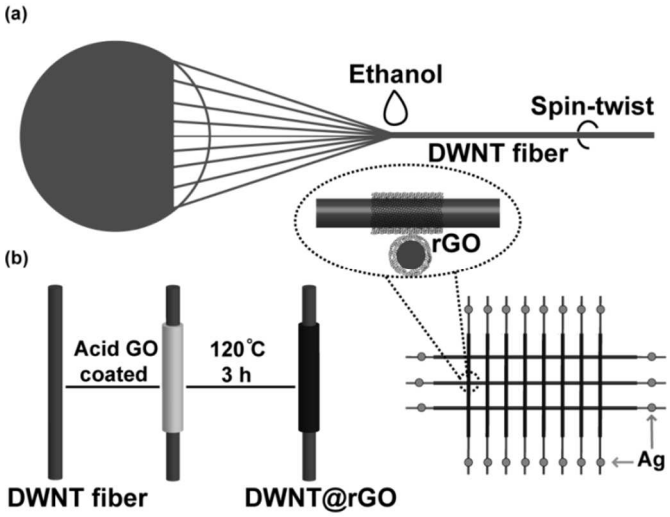

Figure 1. (a) Schematic diagram of the spinning procedure of the formation of DWNT fibers, and (b) the fabrication procedure of the DWNT@rGO all-carbon fibrous woven memories

Figure 1 shows the fabrication procedure of the all-carbon fibrous woven memory. First, DWNT fibers were prepared using a spin-twist method based on our previous work (Figure 1a).[23] The height of our spinnable CNT array is approximately 220 μm and the DWNTs are well aligned in the vertical direction (Supporting information, Figure S1a). Transmission electron microscopy (TEM) image reveals the average diameter of DWNTs is approximately 5

nm (Figure S1b). Briefly, a DWNT film was drawn from the spinnable CNT array and then, by introducing twisting and ethanol densification simultaneously, shrank into a highly densified flexible fiber, leading to a typical strength of 1 GPa and conductivity of $1 \times 10^4\ \mathrm{S \cdot m^{-1}}$.[24] Second, the as-prepared DWNT fibers were coated with a thin layer of acid GO (HNO_3 added with pH=1) through a dip-coating process, as shown in Figure 1b (see the Experimental Section for details). Then, the DWNT@GO fibers were heated at 120 ℃ for 3 h to reduce the GO layer. Finally, silver paste was used for ohmic electrical connection.[7]

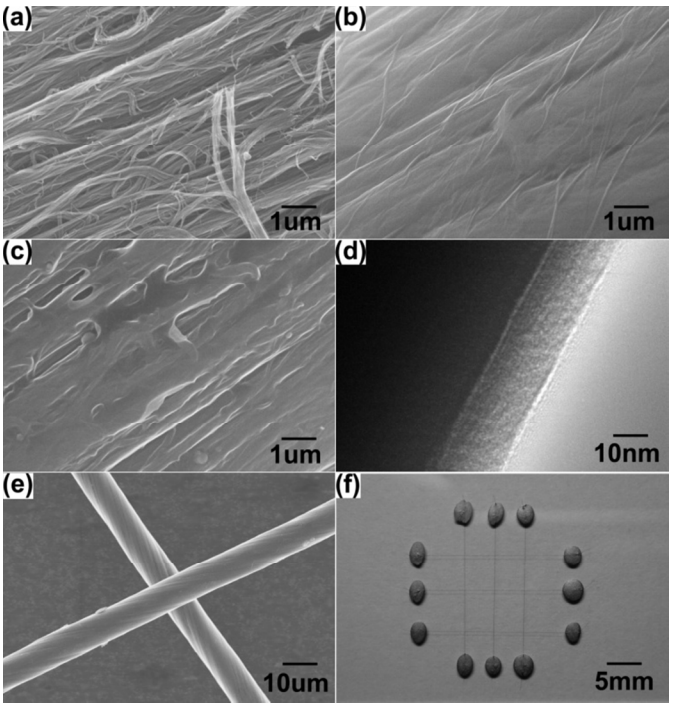

Figure 2. SEM images of (a) the surface morphologies of a pristine DWNT fiber, (b) a DWNT@GO fiber, (c) a DWNT@rGO fiber. (d) TEM image of the rGO layer coated on the DWNT fiber. (e) SEM image of DWNT@rGO fiber device at the cross area. (f) Photograph of the fabricated DWNT@rGO based all-carbon fibrous woven memories.

Scanning electronic microscope (SEM) was used to characterize the morphologies of the DWNT@rGO fibers and the all-carbon fibrous memory, as shown in Figure 2. Thanks to the twisting and ethanol densification process, the obtained DWNT fiber is shape uniform with a diameter of 10 μm (Figure S2). Prior to coating of GO, the DWNT fiber exhibited a densely packed, bundle aligned rough surface feature (Figure 2a). In comparison, after coating of GO, the surface of the DWNT@GO fiber became smooth. In addition, no morphology variation was observed when the DWNT@GO fiber was bended many times (Figure S3), indicating a good interface adhesion between DWNT fiber and GO; the GO wrinkles, raised from thermal fluctuations during coating process,[25] fully covered the fiber surface (Figure 2b). However, the wrinkle features disappeared after reducing GO through a heat process (Figure 2c). TEM image reveals the typical thickness of the rGO layer is 10-20 nm (Figure 2d).

The all-carbon fibrous woven memory was created, as a proof of concept, based on flexible DWNT fibers as electrodes and acid rGO as active material. SEM image of the cross section indicates good contacts between the two DWNT@rGO fibers (Figure 2e). A photograph of the all-carbon fibrous woven memory is shown in Figure 2f, showing the possibility to fabricate e-textiles in the future.

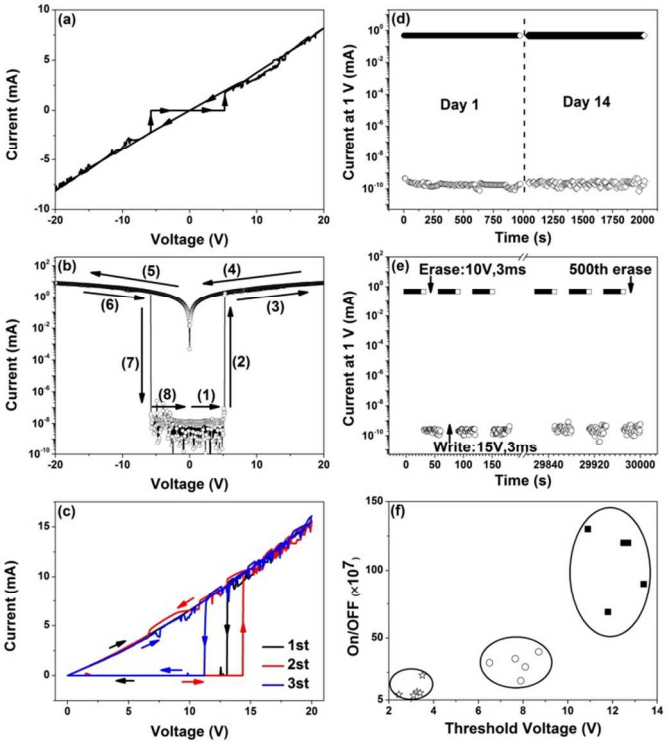

Figure 3. Typical linear (a) and the corresponding semilog (b) *I-V* characteristics of the typical DWNT@rGO fiber all-carbon fibrous woven memory. (c) A bias sweeping sequence that illustrates the memory effect. (d) Retention ability of the all-carbon fibrous woven memory, at a reading voltage of 1 V in the ON and OFF state, in the 1st and 14st day, and the average ON/OFF ratio is 2.8×10^9. (e) Repeatable erase/write operations with pulse voltage, the average ON/OFF ratio is 2.2×10^9. (f) ON/OFF ratio and V_{th} of the all-carbon fibrous woven memory fabricated with different starting GO concentration: 0.8 mg·ml^{-1} (■), 0.4 mg·ml^{-1} (○),0.2 mg·ml^{-1} (☆).

Figure 3a shows the typical linear current-voltage (*I-V*) characteristics of the single one all-carbon fibrous memory, exhibiting a response behavior similar to that of a memristor.[26] Irregular spike features, clearly observed in the *I-V* curves in the voltage range of -20 V to -10 V, and 10 V to 20 V, are considered to be a ubiquitous phenomenon in carbon-based memories.[13] To gain insight into the memory effect, semilog *I-V* result is plotted in Figure 3b, where the arrows represent the sweeping direction of voltage. Initially, a positive voltage swept from 0 to 5.2 V, the all-carbon fibrous memory was in a high resistance state (OFF state), the current during which almost did not change (stage 1). When voltage exceeded the set threshold voltage ($V_{th,SET}$) of 5.2 V, an abrupt current increase occurred from 5.4×10^{-11}A to 1.3×10^{-3}A (stage 2), indicating transition to the low resistance state (ON state), which is equivalent to an erase/write process. The achieved ON/OFF current ratio of 10^7 could compete with the best graphitic memory device using Pt electrodes reported so far.[13] Impressively, the all-carbon fibrous memory retained ON state in the following voltage sweeps (stage 3-6), until to the reset threshold voltage ($V_{th,RESET}$) of -5.8 V, an abrupt current decrease occurred from -2.1×10^{-3}A to -3.8×10^{-11}A, having an ON/OFF current ratio of 10^7. We found the all-carbon fibrous memory has memory effects, that is, the *I-V* behavior depends on whether the previous scan was left in an OFF or

ON state, which is shown in Figure 3c. During the 1st bias sweeping from 0 to 20 V, the device was initially in the ON state and then transferred to the OFF state. However, during the 2st bias sweeping under the same conditions, the device started in the OFF state, as it ended in the previous scan, and the ON state was restored finally. In the 3st scan, the device again started in ON state, because it ended in the ON state previously, and then transferred to the OFF state. The results reveal that the all-carbon fibrous memory can be switched between ON and OFF state through bias sweep routines, which can be used to storage '1' and '0' codes in the ON and OFF states, respectively.

The basic parameters of importance to the performance of memory include ON/OFF current ratio, switching threshold voltage (V_{th}) and retention ability. To study the retention ability, two typical devices are set to ON and OFF states in ambient condition, respectively, and the current-time data were collected in the 1st and 14st day at a reading voltage of 1 V in vacuum condition. As shown in Figure 3d, the current of ON and OFF states hardly changed for 1000s and no degradation was observed after 14 days air exposure. Surprisingly, the obtained highest ON/OFF current ratio is larger than 10^9, two orders of magnitude higher than the best reported so far[13]. Furthermore, the memory could also be switched ON and OFF by a pulse voltage (Figure 3e), which also exhibited ultra-high ON/OFF current ratios ($\approx 10^9$) when written by a bias pulse (3 ms) voltage of 15 V and erased by a bias pulse (3 ms) voltage of 10 V, and the devices maintained the same ON/OFF current ratio after 500 write/erase operations, showing superior retention performance. Apparently, the concentration of starting GO should have a direct effect on the ON/OFF ratio and V_{th}, the results were plotted in Figure 3f. At the GO concentration of $0.8\ \mathrm{mg \cdot ml^{-1}}$, the obtained average V_{th} and ON/OFF ratio were 12.2 V and 1.3×10^9, respectively. When the GO concentration was decreased to $0.4\ \mathrm{mg \cdot ml^{-1}}$, we got an average V_{th} of 7.8 V, and an average ON/OFF ratio of 3.1×10^8. Further decreasing the GO concentration to $0.2\ \mathrm{mg \cdot ml^{-1}}$, the average V_{th} and average ON/OFF ratio became 3.14 V and 2.7×10^8, respectively. The data can be reasonably explained that higher concentration of starting GO would form thicker acid rGO layer, leading to larger V_{th} and higher ON/OFF current ratio.

Hitherto, different resistive switching mechanisms have been proposed for carbon memories, e.g., formation and breaking of carbon atomic chains,[9, 13] atomic movement and/or chemical rearrangement[10] that bridge the nano gap junctions in graphene layers; DOS limited contact model in graphene layer;[17] rupture and formation of conducting filaments between graphene oxide and reactive metal electrodes, Al, e.g.;[11, 18] reversible thermal-assisted reduction and oxidation of graphene oxide;[16] desorption/absorption of oxygen-related groups on the GO sheets as well as the diffusion of the top electrodes;[12, 15] migration of oxygen in the GO layer[7, 27] and so on, showing the complexity in carbon based resistive switching process. Generally speaking, the electrodes used in carbon based memories can be classified into two types: the reactive electrodes (Al) and non-reactive electrodes (Pt, Au, and Carbon). For reactive electrodes (Al), graphene oxide is (GO) used, it is believed that rupture and formation of conducting filaments between graphene oxide and reactive metal electrodes via oxygen migration caused the switching behaviors,[11] if non-reactive electrode (Carbon) is used in GO based memories, the memories then become non-rewritable because of irreversible migration of oxygen.[7] In comparison, for non-reactive electrodes (Pt and Au), the graphene or reduced graphene (rGO) is used, the switching mechanism is believed to be the formation and breaking of carbon atomic chains between graphene nanogaps, and the memories are rewritable.[9] Considering our all-carbon memories consisting of non-reactive carbon electrodes and rGO active switching materials, and the memories are rewritable, the switching mechanism should be similar to that of the memories using Pt or Au electrodes, that is to say, the reversible formation and breaking of carbon atomic chains between graphene nanogaps.

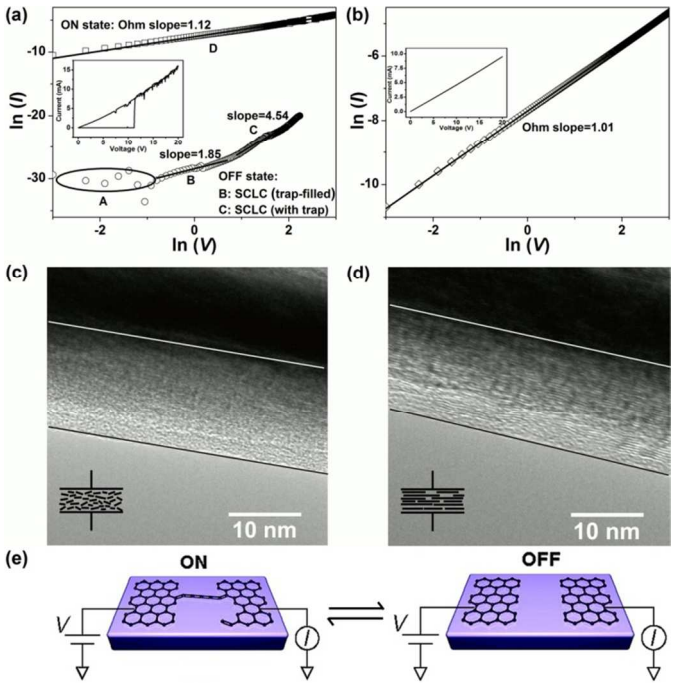

Figure 4. (a) The log-log plot of the typical *I-V* characteristics of the all-carbon fibrous woven memory that shows resistive switching (inset: linear plot) and (c) the corresponding TEM characterization (inset: the disorder rGO drawing). (b) The log-log plot of the typical *I-V* characteristics of the all-carbon fibrous woven memory that do not switch (inset: linear plot); and (d) the corresponding TEM characterization (inset: the regular rGO drawing). (e) The possible schematic of the switching mechanism between disorder graphene layers, Reproduced with permission from ref. 9. ©2008 American Chemical Society.

In our experiments, we found that starting acid GO solution (pH=1) is necessary, thus HNO_3 is intentionally added. If pristine GO solution (pH=4-6) is used, no switching behaviors can be observed. To explore the effects of the HNO_3 on the rGO structure and the subsequently memories' performance, TEM combined *I-V* analysis was employed, the results are displayed in Figure 4. Two devices, one has resistive switching behaviors (made with pH=1 acid GO solution) while the other one not (made with pH=5 pristine GO solution), have been investigated. For the devices do not switch, 'ohmic like' behavior (Figure 4b) and a regular rGO structure (Figure 4d, TEM image) were observed. In comparison, the memory with resistive switching behaviors have a disorder rGO structure (Figure 4c, TEM image) and behave very different in the OFF and ON states (Figure 4a), that is 'space charge region-limited' and 'ohmic like' conducting behaviors in the OFF and ON state, respectively. As the starting GO solution is in low pH state (pH=1), the carboxyl groups is protonated such that the GO sheets became less hydrophilic and easy to form aggregates,[29] facilitating the disorder rGO structure formation during heat-treating process, in which exists many graphene nanogaps and edges (inset of Figure 4c). However, if the pH of the starting GO solution lies in the range of 4-6, the carboxyl groups are slightly protonated such that the GO sheets are prefer to dissolve, thus the regular rGO structure may be more favourable during heat process, in which the graphene

nanogaps and edges are not easy to form (inset of Figure 4d).The 'space charge region-limited' behavior in OFF state can be divided into three stages, marked A, B and C in Figure 4a. Stage A gives no results due to test limitation, stage B exhibits a slop of $1.85 \approx 2$, indicating a trap-filled "space charge region-limited" behavior, and stage C shows a slope of $4.54 > 2$, presenting a with-trap "space charge region-limited" behavior, coinciding with the disorder rGO structure conducting mechanism reported by others[7]. Upon the basis of our TEM observations and *I-V* results, consider the rewritable property and non-reactive of the CNT fiber electrodes, we infer that the disorder rGO layer, in which might exist graphene nano gaps and edges that can be bridged by carbon atomic chains,[9, 10, 13, 28] should be responsible for the resistive switching process, shown as Figure 4e.

Conclusions

In summary, as a proof of concept, we have fabricated the all-carbon fibrous woven memory formed by acid rGO-coated DWNT fibers and systematically studied their memory effects. The disorder rGO was believed to act as switching materials, and the flexible DWNT fiber that was directly spin-twisted from spinnable CNT array served as electrode. Though a better understanding of the mechanism would be helpful, what are presently apparent are the unique memory properties of the woven devices, the electric bistability, resilience, nonvolatility, unprecedented ultra-high ON/OFF ratios of 10^9, switching times to the tested 3 ms, combined with predictable, simple two-terminal geometry and woven morphology, make them attractive structures for future wearable electronics.

Experimental section

The detailed double-walled carbon nanotube (DWNT) and fiber spin-twisted procedure was described in our previous studies.[30] Spinnable DWNT arrays were synthesized in a 5 inch-diameter quartz tube at 750 ℃ for 15 minutes by chemical vapour deposition (CVD). Argon and ethylene were used as the carrier gas and the carbon source, respectively. The catalyst was prepared by sequence depositing 20 nm Al_2O_3 and 0.8 nm Fe on SiO_2/Si substrate by electron-beam technique. The DWNT fibers were spun from the as-prepared CNT array with a blade first, and ethanol was applied to densify the fiber to obtain a smooth surface during the spin-twisted procedure.

Graphene oxide (GO) was prepared from graphite powder by a modified Hummers method.[31] The as-prepared GO powder was re-dispersed in water at 0.8 , 0.4 and $0.2\ \mathrm{mg \cdot ml^{-1}}$ by strong ultrasonication more than 30 min, respectively. HNO_3 was added to obtain acid GO (pH=1) solutions to protonate the carboxyl groups such that the GO sheets became less hydrophilic to form aggregates. Then the DWNT fibers were immersed in acid GO solutions for 2 h, and then dried under ambient conditions. After that, the DWNT@GO fibers were heat at 120 ℃ for 3 h to reduce the GO layer. Finally, the all-carbon fibrous woven memories were formed by cross stacking two DWNT@rGO fibers at a right angle.

Scanning electron microscope (SEM) images and transmission electron microscopy (TEM) images were collected with field-emission scanning electron microscope (Hitachi, S4800) and FEI Tecnai G2 F20 S-Twin, 200 kV, respectively. *I-V* measurements were conducted by using a Keithley 4200 semiconductor parameter analyser at room temperature under a vacuum of $\sim 5 \times 10^{-3}$ mm Hg.

Acknowledgements

The work was sponsored by the National Natural Science Foundation of China (No. 21273269, 10834004), National Basic Research Program of China (No. 2011CB932600, 2012CB932402), and Knowledge Innovation Program (No. KJCX2.YW.M12) by the Chinese Academy of Sciences.

Notes and references

1. M. Hamedi, R. Forchheimer and O. Inganas, *Nat. Mater.*, 2007, **6**, 357-362.
2. M. Hamedi, L. Herlogsson, X. Crispin, R. Marcilla, M. Berggren and O. Inganas, *Adv. Mater.*, 2009, **21**, 573-577.
3. H. Lin, W. Weng, J. Ren, L. Qiu, Z. Zhang, P. Chen, X. Chen, J. Deng, Y. Wang and H. Peng, *Adv. Mater.*, 2014, **26**, 1217-1222.
4. Z. B. Yang, J. Deng, X. L. Chen, J. Ren and H. S. Peng, *Angew. Chem., Int. Ed.*, 2013, **52**, 13453-13457.
5. M. R. Lee, R. D. Eckert, K. Forberich, G. Dennler, C. J. Brabec and R. A. Gaudiana, *Science*, 2009, **324**, 232-235.
6. X. Fang, Z. B. Yang, L. B. Qiu, H. Sun, S. W. Pan, J. Deng, Y. F. Luo and H. S. Peng, *Adv. Mater.*, 2014, **26**, 1694-1698.
7. G. Sun, J. Liu, L. Zheng, W. Huang and H. Zhang, *Angew. Chem., Int. Ed.*, 2013, **52**, 13351-13355.
8. S. T. Han, Y. Zhou and V. A. Roy, *Adv. Mater.*, 2013, **25**, 5425-5449.
9. B. Standley, W. Bao, H. Zhang, J. Bruck, C. N. Lau and M. Bockrath, *Nano letters*, 2008, **8**, 3345-3349.
10. H. Zhang, W. Z. Bao, Z. Zhao, J. W. Huang, B. Standley, G. Liu, F. L. Wang, P. Kratz, L. Jing, M. Bockrath and C. N. Lau, *Nano letters*, 2012, **12**, 1772-1775.
11. H. Y. Jeong, J. Y. Kim, J. W. Kim, J. O. Hwang, J. E. Kim, J. Y. Lee, T. H. Yoon, B. J. Cho, S. O. Kim, R. S. Ruoff and S. Y. Choi, *Nano letters*, 2010, **10**, 4381-4386.
12. C. L. He, F. Zhuge, X. F. Zhou, M. Li, G. C. Zhou, Y. W. Liu, J. Z. Wang, B. Chen, W. J. Su, Z. P. Liu, Y. H. Wu, P. Cui and R. W. Li, *Appl. Phys. Lett.*, 2009, **95**.
13. Y. Li, A. Sinitskii and J. M. Tour, *Nat. Mater.*, 2008, **7**, 966-971.
14. A. Sinitskii and J. M. Tour, *ACS Nano*, 2009, **3**, 2760-2766.
15. F. Zhuge, W. Dai, C. L. He, A. Y. Wang, Y. W. Liu, M. Li, Y. H. Wu, P. Cui and R. W. Li, *Appl. Phys. Lett.*, 2010, **96**.
16. C. L. He, Z. W. Shi, L. C. Zhang, W. Yang, R. Yang, D. X. Shi and G. Y. Zhang, *ACS Nano*, 2012, **6**, 4214-4221.
17. X. M. Wang, W. G. Xie, J. Du, C. L. Wang, N. Zhao and J. B. Xu, *Adv. Mater.*, 2012, **24**, 2614-2619.
18. S. M. Jilani, T. D. Gamot, P. Banerji and S. Chakraborty, *Carbon*, 2013, **64**, 187-196.
19. N. Behabtu, C. C. Young, D. E. Tsentalovich, O. Kleinerman, X. Wang, A. W. K. Ma, E. A. Bengio, R. F. ter Waarbeek, J. J. de Jong, R. E. Hoogerwerf, S. B. Fairchild, J. B. Ferguson, B. Maruyama, J. Kono, Y. Talmon, Y. Cohen, M. J. Otto and M. Pasquali, *Science*, 2013, **339**, 182-186.
20. K. Koziol, J. Vilatela, A. Moisala, M. Motta, P. Cunniff, M. Sennett and A. Windle, *Science*, 2007, **318**, 1892-1895.
21. Y. Zhang, W. Bai, X. Cheng, J. Ren, W. Weng, P. Chen, X. Fang, Z. Zhang and H. Peng, *Angew. Chem., Int. Ed.*, 2014, **53**, 14564-14568.
22. J. Zhao, X. Zhang, J. Di, G. Xu, X. Yang, X. Liu, Z. Yong, M. Chen and Q. Li, *Small*, 2010, **6**, 2612-2617.
23. Q. W. Li, X. F. Zhang, R. F. DePaula, L. X. Zheng, Y. H. Zhao, L. Stan, T. G. Holesinger, P. N. Arendt, D. E. Peterson and Y. T. Zhu, *Adv. Mater.*, 2006, **18**, 3160-3163.
24. F. Meng, X. Zhang, R. Li, J. Zhao, X. Xuan, X. Wang, J. Zou and Q. Li, *Adv. Mater.*, 2014, **26**, 2480-2485.
25. A. Fasolino, J. H. Los and M. I. Katsnelson, *Nat. Mater.*, 2007, **6**, 858-861.
26. E. Linn, R. Rosezin, C. Kugeler and R. Waser, *Nat. Mater.*, 2010, **9**, 403-406.
27. L.-H. Wang, W. Yang, S. Qing-Qing, P. Zhou, H.-L. Lu, S.-J. Ding and D. W. Zhang, *Appl. Phys. Lett.*, 2012, **100**, 063509-063509-063504.
28. O. Cretu, A. R. Botello-Mendez, I. Janowska, C. Pham-Huu, J. C. Charlier and F. Banhart, *Nano letters*, 2013, **13**, 3487-3493.

29. C. J. Shih, S. Lin, R. Sharma, M. S. Strano and D. Blankschtein, *Langmuir : the ACS journal of surfaces and colloids*, 2012, **28**, 235-241.
30. J. Di, D. Hu, H. Chen, Z. Yong, M. Chen, Z. Feng, Y. Zhu and Q. Li, *ACS Nano*, 2012, **6**, 5457-5464.
31. V. C. Tung, M. J. Allen, Y. Yang and R. B. Kaner, *Nat Nano*, 2009, **4**, 25-29.

[a] Key Lab of Nanodevices and Applications, Suzhou Institute of Nano-Tech and Nano-Bionics, Chinese Academy of Sciences (CAS), Ruoshui Road 398, Suzhou, 215123, China, qwli2007@sinano.ac.cn.

[b] University of Chinese Academy of Science, Yuquan Road 19, Beijing, 100049, China.

†Electronic Supplementary Information (ESI) available: [details of any supplementary information available should be included here]. See DOI: 10.1039/c000000x/